---

**Proceedings Paper:**
Nie, Y., Ko, P. and Drummond, R. orcid.org/0000-0002-2586-1718 (2024) Optimal flight trajectories of hybrid electric aircraft with in-flight charging. In: 2024 European Control Conference (ECC) Proceedings. 2024 European Control Conference (ECC), 25-28 Jun 2024, Stockholm, Sweden. Institute of Electrical and Electronics Engineers (IEEE) , pp. 218-223. ISBN 9798331540920

https://doi.org/10.23919/ecc64448.2024.10590832

---

# Optimal Flight Trajectories of Hybrid Electric Aircraft with In-flight Charging

Yuanbo Nie, Paing Ko and Ross Drummond *Dept. of Automatic Control and Systems Engineering*
*University of Sheffield*
Sheffield, UK
{y.nie, phmuko1, ross.drummond}@sheffield.ac.uk

***Abstract*— The transition towards electric aircraft is particularly challenging due to the relatively low specific energy densities of electrical energy storage systems. If electric aircraft are to be realised, flight paths must be optimised to take advantage of the unique features of electric propulsion systems. In this paper, the problem of determining the optimal flight trajectories for aircraft powered by a combination of a fuel cell stack and lithium-ion battery pack is considered. Particular emphasis is given to the role of the battery pack's temperature and in-flight charging requirements on the results. Solutions that minimise the fuel consumption and the flight time are first considered. For both cases, the optimal solution was observed to discharge the battery during the climb with only minimal in-flight recharging of the battery by the fuel cell. A scenario that requires a fast climb and descent and the battery to be charged upon arrival was identified and shown to lead to an oscillatory profile for optimal in-flight charging. These results demonstrate the potential of solving optimal control problems to generate tailored electric aircraft trajectories.**

Electric aircraft, trajectory optimisation, optimal control theory, numerical methods.

## I. Introduction

Whilst the roll out of electric vehicles (EVs) is gathering momentum, progress in the decarbonisation of aviation has been much slower. Even though the aviation sector only accounts for a small proportion of total greenhouse gas emissions (for example, during 2022 in the UK, aviation was responsible for 26.0 $MtCO_{2e}$ whereas the transport sector as a whole was responsible for 112.5 Mt [8]), emissions from aircraft are predicted to grow in the future and high altitude aviation is understood to contribute to an extra greenhouse effect due to the formation of persistent condensation trails (contrails) [8].

To counter this increase in pollution, there has been a push to develop electric aircraft charged by renewable energy sources. Several prototype electric aircraft are now entering the testing stage such as the Rolls-Royce ACCEL aircraft which reached a speed of 480 km/h. Such prototype electric aircraft are impressive, and demonstrate how significant progress can be made by leveraging the recent advances in electrical energy storage, notably in battery technology and charging infrastructure, stimulated by the explosive growth in electric vehicles. However, in contrast to the growing adoption of electric vehicles by the public, current electric aircraft have yet to break out from the prototype stage and widespread adoption remains only on the horizon.

The sobering reasons behind the sluggishness in switching to electric aircraft are simply that, currently, their performance can not match fossil-fueled powered aircraft and they are less well-understood. For example, the battery-powered Heart Aerospace ES-19 regional aircraft only has a planned range of 400 km with 19 passengers, whereas a similar turboprop counterpart can easily fly missions beyond 1000 km. Besides their increased costs, the main obstacles for aircraft electrification are: i) the relatively low specific energy and power densities of current electrical energy devices, ii) safety fears around fires (with Li-ion battery fires being particularly dangerous), and iii) the lack of airport charging infrastructure to facilitate rapid aircraft turnaround. The aggressive power/energy demands of aircraft means that any performance limitations in the power sources are exacerbated compared to EVs (which are currently seeing a switch to low cost, low energy density systems with the rise of Na-ion and $LiFePO_4$ batteries, neither of which are suitable for long-rage aviation).

There is then a need to optimise the design and flight paths of current electric aircraft [3]. Electric aircraft and traditional aircraft have significantly different characteristics (for example, traditional aircraft get lighter during the flight as they burn fuel whereas batteries do not as charge is just transferred from the cathode to the anode) and these differences need to be accounted for in how the aircraft is flown. Addressing this problem is the focus of this paper. A method to optimise the flight trajectory of an electrified Fokker 50 aircraft with a hybrid power system is described. It is assumed that the power source of this electric is formed of a battery pack and a fuel cell stack and a short-haul flight from London to Berlin is considered. The main results of the paper are:

1) Optimal flight trajectories are generated for electric aircraft powered by a combination of a lithium-ion battery pack and a fuel cell stack.
2) Only limited in-flight charging of the battery pack is observed for minimum time and minimum propellant consumption problems.
3) Oscillations in the in-flight charging response were observed for problems where the aircraft was encouraged to maintain a high altitude flight and the battery pack

Ross Drummond was supported by a UK Intelligence Community Research Fellowship from the Royal Academy of Engineering.

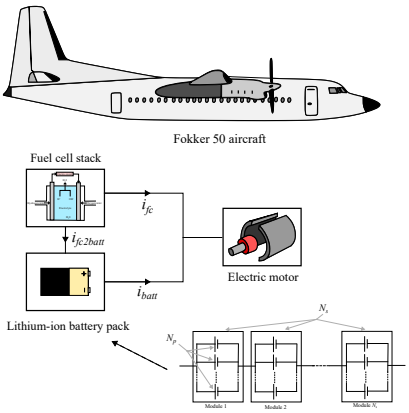


Fig. 1: Illustration of the modelled electric Fokker 50 aircraft.

was to be charged on arrival.

4) Insulating the battery pack from the drop in atmospheric temperature can significantly improve performance.

The `ICLOCS2` Toolbox [16] for `MATLAB` was used to numerically solve the optimal control problems for the flight trajectories using the direct transcription method of direct collocation. The results highlight the differences between optimal flight paths for electrified and traditional turboprop powered aircraft, with significant scope for further development and experimentation.

Several other recent studies have considered the optimal management of electric aircraft. For example, [12] used the minimum principle to generate optimal flight paths and a similar approach was used in [13] for hydrogen powered aircraft while ADMM based solvers were used in [9] and [10] for hybrid aircraft with fossil fuel components. There has also been interesting studies exploring how features of the battery pack affect electric aircraft; for example [11] showed the importance of including thermal cooling of the pack, [20] examined the role of charging the battery in flight, [19] highlighted how the battery model's fidelity affected the solutions, and [15] showed the impact of pack topology on the response. Recently, there have also been more fundamental battery research for electric aircraft, such as the modelling results of [6], the performance requirements [5] and the aviation-focused battery degradation dataset of [4].

Whilst there are similarities between the presented results and these papers (specifically, on the use of optimal control theory to generate flight paths for aircraft powered by batteries), there are also important differences. Most significant is the paper's focus on hybrid battery/fuel cell power systems, as opposed to the common hybrid battery/turboprop arrangements of papers such as [10]. We also explore how aspects such as the battery pack end state-of-charge and its thermal response affect the solution. Specifically, a flight scenario prioritising the aircraft to remain at high altitude and the battery to be charged at the end of flight is shown to generate oscillatory profiled for optimal in-flight charging. This is in contrast with traditional understanding based on minimum propellant consumption and minimum time solutions that in-flight charging of the battery provides limited benefits [20]. Moreover, the usefulness of numerical optimal control for solving such problems at scale is demonstrated. We are conscious that these results are preliminary and can be expanded upon significantly, for example by incorporating more advanced battery models, such as packs of Doyle-Fuller-Newman models which go beyond the single particle models of [19]. Doing so will enable higher fidelity simulations able to account for effects such as cell-to-cell variability in the pack and degradation due to lithium plating.

## II. Aircraft Model

We begin by introducing the aircraft model used for the flight trajectory optimisation. As illustrated in Figure 1, a Fokker 50 was chosen as the representative aircraft to be optimised. This aircraft is a regional Turboprop airliner able to seat 40-70 passengers with specifications given in [1].

### A. Aircraft dynamics

The following point mass model from [17], modified from Cartesian coordinates to latitude and longitude states, is used to describe the dynamics of the aircraft:

$$\dot{h}(t) = v_{\text{TAS}}(t)\sin(\gamma(t)) \tag{1a}$$

$$\dot{\nu}(t) = \frac{v_{\text{TAS}}(t)\cos(\gamma(t))\cos(\chi(t)))}{R_{\text{E}} + h(t)}, \tag{1b}$$

$$\dot{\bar{\omega}}(t) = \frac{v_{\text{TAS}}(t)\cos(\gamma(t))\sin(\chi(t)))}{(R_{\text{E}} + h(t))\cos(\nu(t))}, \tag{1c}$$

$$\begin{aligned}\dot{v}_{\text{TAS}}(t) = &\frac{1}{m(t)}(F_n(v_{\text{CAS}}(t), h(t), \Gamma(t)) \\ &- D(v_{\text{TAS}}(t), h(t), \alpha(t)) - m(t)g\sin(\gamma(t)))\end{aligned} \tag{1d}$$

$$\begin{aligned}\dot{\gamma}(t) = &\frac{1}{m(t)v_{\text{TAS}}(t)}(L(v_{\text{TAS}}(t), h(t), \alpha(t))\cos(\phi(t)) \\ &- m(t)g\cos(\gamma(t)))\end{aligned} \tag{1e}$$

$$\dot{\chi}(t) = \frac{L(v_{\text{TAS}}(t), h(t), \alpha(t))\sin(\phi(t))}{\cos(\gamma(t))m(t)v(t)} \tag{1f}$$

$$\dot{m}(t) = -F_e(h(t), v_{\text{CAS}}(t), \Gamma(t)). \tag{1g}$$

The model's states are: altitude ($h$), latitude($\nu$), longitude ($\bar{\omega}$), true airspeed ($v_{\text{TAS}}$), flight path angle ($\gamma$), tracking angle ($\chi$), aircraft weight ($m$). The control inputs are the throttle position ($\Gamma$), the angle of attack ($\alpha$) and the roll angle ($\phi$). $v_{\text{CAS}}$ is the calibrated airspeed which is converted from $v_{\text{TAS}}$ using atmospheric conditions. The earth's radius is taken to be $R_E = 6.371 \times 10^6$ km and $g = 9.81$ m/s$^2$ is the gravitational acceleration. The computation of thrust $F_n$, lift $L$ and drag $D$ and the fuel flow $F_e$ involves the aerodynamic and propulsion modelling from the performance data [7].

## III. Hybrid electric power system

In this section, the model for the electric propulsion system of this hybrid aircraft is described. The Fokker 50 aircraft was assumed to be powered by the hybrid power source of Figure 1 where the current to the motor is the sum of that

from both the fuel cell and the battery. Since the fuel cell capacity is much larger than the battery, the fuel cell is also assumed to be able to re-charge the battery during the flight.

### A. Fuel cell model

A model from [14] is used to describe the fuel cell, with state equations

$$\dot{V}_{\text{act}}(t) = -\frac{3}{T_d}V_{\text{act}}(t) + A_{\text{fc}} \ln\left(-\frac{i_{\text{fc}}(t)}{i_0}\right), \tag{2a}$$

$$\dot{m}(t) = \left(-\frac{M_{H_2}}{2F} - \frac{M_{\text{Air}}}{4FM_f}\right) i_{\text{fc}}(t) N_{\text{fc}}. \tag{2b}$$

Here, $V_{\text{act}}$ is the instantaneous voltage, $A_{\text{fc}}$ is the activation voltage reaction rate variable, $i_{\text{fc}}$ is the fuel cell current, $i_0 = 50$ A is the exchange current density, $\tau_d = 1$ s is the time constant for the activation voltage drop. Additionally, $M_{H_2} = 1.00794 \times 2 \times 10^{-3}$ kg mol$^{-1}$ is the molar mass of liquid hydrogen, $M_{\text{Air}} = 28.96 \times 10^{-3}$ kg mol$^{-1}$ is the molar mass of air, $M_f = 0.209476$ is the molar fraction of oxygen in air, $F = 96485.3$ C mol$^{-1}$ is Faraday's constant and $N_{\text{fc}} = 5000$ is the number of series-connected cells in the stack.

The fuel cell voltage is described by

$$V_{\text{fc}}(t) = N_{\text{fc}}\left(V_{\text{oc,fc}}(t) - (V_{\text{act}}(t) + V_{\text{oh}}(t) + V_{\text{t}}(t))\right) \tag{2c}$$

where $V_{\text{oh}}$ is the voltage drop due to the fuel cell's internal resistance, $V_{\text{oc,fc}} = 1.2$ V is the open circuit voltage for a single cell, and $V_{\text{transport}}$ is the voltage drop due to reactant mass transport across the fuel cell. These additional voltage drops satisfy

$$V_{\text{oh}}(t) = -R_{\text{i}} i_{\text{fc}}(t), \tag{2d}$$

$$V_{\text{t}}(t) = m_t e^{-n_t i_{\text{fc}}(t)}, \tag{2e}$$

with $R_i = 0.9 \times 10^{-3}\,\Omega$ the fuel cell internal resistance, and $m_t = 3 \times 10^{-5}$ V and $n_t = 0.015$ A$^{-1}$ some empirical constants for transport losses.

### B. Battery Model

An equivalent circuit model is used to capture the dynamics of the lithium-ion battery of the hybrid aircraft, as shown in Figure 2. It is assumed that a current can be drawn from the fuel cell stack to charge the battery, giving the overall charging current of $i_{\text{batt,tot}}(t) = i_{\text{batt}}(t) - i_{\text{fc2batt}}(t)$ where $i_{\text{batt}}(t)$ is the current (with signs taken to be positive for charging and negative for discharging) drawn from the battery and $i_{\text{fc2batt}}(t)$ is the current from the fuel cell to charge the battery in flight. As the voltages are different for the two energy systems, the conversion from the fuel-cell discharge current to the battery charging current will be based on the exchanged power with an efficiency of $\eta = 0.8$. The model equations for the battery pack are obtained from [18] which were parameterised for the A123 Systems APR18650M1A' high power lithium-iron phosphate cylindrical cells of [2]. The electrical equations of a multi-cell battery pack based

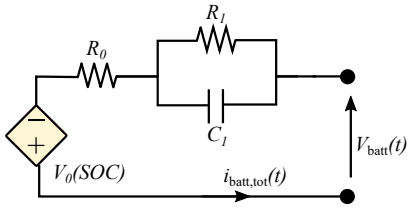


Fig. 2: Equivalent circuit model of the battery.

on this model are

$$\dot{x}_1 = \frac{i_{\text{batt,tot}}(t)}{N_p Q}, \quad \dot{x}_2 = -\frac{x_2(t)}{R_1 C_1} + \frac{i_{\text{batt,tot}}(t)}{N_p C_1}, \tag{3a}$$

$$V_{\text{batt}}(t) = N_s\left(V_0(x_1(t)) + x_2(t) + R_0\frac{i_{\text{batt,tot}}(t)}{N_p}\right), \tag{3b}$$

with $x_1(t)$ being the state-of-charge of the cell, $x_2(t)$ the relaxation voltage of the RC pair in Figure 2, and $V_{\text{batt}}(t)$ is the cell voltage. As illustrated in Figure 1, the pack is built from modules of $N_p = 100$ cells connected in parallel, and with $N_s = 200$ of these modules then connected in series. This model assumes that all cells in the pack are the same, and so the current is distributed evenly across the module's parallel branches. The model parameters are: $Q = 3$Ah is the cell capacity, $R_0 = 0.003\Omega$ is the series resistance, and the RC-pair is defined by $R_1 = 0.002\Omega$, $C_1 = 8 \times 10^3$F. A look-up table is used to compute the open-circuit voltage (OCV) $V_0$ from the state-of-charge $x_1$ based on the experimental data from [2], [18].

The temperature dynamics of this cell are modelled as

$$\begin{aligned} m_{\text{batt}} C_p \Delta\dot{T}_{\text{batt}}(t) = &- h_{\text{batt}} A_{\text{batt}} \Delta T_{\text{batt}}(t) \\ &+ R_0(i_{\text{batt}}(t)^2 + i_{\text{fc2batt}}(t)^2) \\ &+ x_2(t)(i_{\text{batt}}(t) - i_{\text{fc2batt}}(t)) \end{aligned} \tag{3c}$$

where $\Delta T_{\text{batt}}(t) = T_{\text{batt}}(t) - T_{\text{amb}}(t)$ [K] is the temperature difference between the cell $T_{\text{batt}}(t)$ and the ambient air surrounding the pack $T_{\text{amb}}(t)$. When the pack is insulated, then $T_{\text{batt}}(t) = 293$ K and when it is not, then $T_{\text{amb}}(t)$ decreases with altitude following the standard atmospheric condition. $m_{\text{batt}} = 39 \times 10^{-3}$ kg is the cell mass, $C_p = 2025.737$ Jkg$^{-1}$K$^{-1}$ is the specific heat capacity, $A_{\text{batt}} = 3.714 \times 10^{-3}$ m$^2$ is the surface area and $h_{\text{batt}} = 43$ W m$^{-2}$K$^{-1}$ is the convective heat transfer coefficient. The entropic heat generation rate has been neglected in this model as it is assumed that the large currents during electric flight cause joule heating to dominate.

### C. Integrating Battery and Fuel Cells

The electric motor is modelled as a first-order response, with the dynamics of the shaft power being

$$\dot{P}_{\text{w,shaft}} = \frac{P_{\text{w,total}} - P_{\text{w,shaft}}}{\tau_m} \tag{4a}$$

and $\tau_m = 2$ s is the time constant. $P_{\text{w,total}}$ is the total power available from this hybrid power system, defined as

$$P_{\text{w,total}} = -(V_{\text{batt}} i_{\text{batt}} + V_{\text{fc}} i_{\text{fc}}). \tag{4b}$$

## IV. Trajectory Optimisation and Results

The benchmark flight scenario considered in this work is from London to Berlin. This flight scenario has a duration of approximately 2 hours starting from the acceleration altitude (end of take-off phase) and lasting till the final approach (before landing).

### A. Traditional Trajectory Optimisation Problem

The problem of optimising the flight trajectories for the electric aircraft modelled by eqs. (1) to (4) is considered. Two traditional problems were solved; one minimising the consumption of the propellant, i.e. maximising the final mass of the aircraft with a fixed initial mass

$$\min_{x,u,t_f} -m(t_f) + J_{\text{reg}} \tag{5}$$

and another formulation minimising the flight time

$$\min_{x,u,t_f} t_f + J_{\text{reg}} \tag{6}$$

with $J_{\text{reg}} = \int_0^{t_f} \lambda_\phi \phi(t)^2 + \lambda_\gamma \gamma(t)^2 + \lambda_i((\frac{di_{\text{batt}}}{dt})^2 + (\frac{di_{\text{fc}}}{dt})^2 + (\frac{di_{\text{batt2fc}}}{dt})^2)\ \mathrm{d}t$ a regularisation cost, with regularisation weights $\lambda_\phi = 1$, $\lambda_\gamma = 100$ and $\lambda_i = 0.01$ chosen such that $J_{\text{reg}} \ll |-m(t_f)|$ and $J_{\text{reg}} \ll t_f$. The optimisation problems have 12 state variables with $x = [h, \nu, \bar{\omega}, v_{\text{TAS}}, \gamma, \chi, m, P_{\text{w,shaft}}, x_1, x_2, V_{\text{act}}, T_{\text{batt}}]^\top$ and 5 input variables with $u = [\Gamma, \alpha, \phi, i_{\text{batt}}, i_{\text{fc}}, i_{\text{fc2batt}}]^\top$. The final time of the solution $t_f$ is free therefore it is also a decision variable. The optimisation problems are solved subject to dynamics constraints eqs. (1) to (4) and additional path and boundary constraints for the aircraft:

$$\begin{aligned}
&487.68 < h(t) < 7620\,[m],\ 89.50 \le v_{\text{TAS}}(t) \le 212.28\,[m/s],\\
&0 \le P_{\text{w,shaft}}(t) \le 5000\,[kW],\ 14000 \le m(t) \le 18000\,[kg],\\
&0 \le \Gamma(t) \le 1\,,\ -10 \le \alpha(t) \le 10\,[^\circ],\ 45 \le \phi(t) \le 45\,[^\circ],\\
&h(0) = 487.68\,[m],\ v_{\text{TAS}}(0) = 89.5\,[m/s],\ m(0) = 18\,[t],\\
&\nu(0) = 51.47\,[^\circ],\ \bar{\omega}(0) = -0.4543\,[^\circ],\ \gamma(0) = 8\,[^\circ],\\
&\gamma(t_f) = -3\,[^\circ],\ h(t_f) = 609.6\,[m],\ v_{\text{TAS}}(t_f) = 100\,[m/s],\\
&\nu(t_f) = 52.52\,[^\circ],\quad \bar{\omega}(t_f) = 13.405\,[^\circ],
\end{aligned}$$

for the battery:

$$\begin{aligned}
&0.2 \le x_1(t) \le 1,\quad -0.25 \le x_2(t) \le 0.25\,[V],\\
&2.5 \le \frac{V_{\text{batt}}(t)}{N_s} \le 4.5\,[V],\quad -\frac{N_p Q}{720} \le i_{\text{batt}}(t) \le 0\,[A],\\
&x_1(0) = 0.9,\quad x_2(0) = 0\,[V],
\end{aligned}$$

and for the fuel cell:

$$\begin{aligned}
&0 \le V_{\text{act}}(t) \le 1.2\,[V],\quad 0 \le V_{fc}(t),\\
&-600\,[A] \le i_{\text{fc}}(t) + i_{\text{fc2batt}}(t) \le -i_0,\\
&V_{\text{act}}(0) = 0\,[V],\quad x_2(0) = 0\,[V].
\end{aligned}$$

Finally, the charging of the battery by the fuel cell is subject to the constraint

$$-\frac{N_p Q}{720} \le i_{\text{fc2batt}}(t)\frac{V_{\text{fc}}(t)}{V_{\text{batt}}(t)} \le 0\,[A].$$

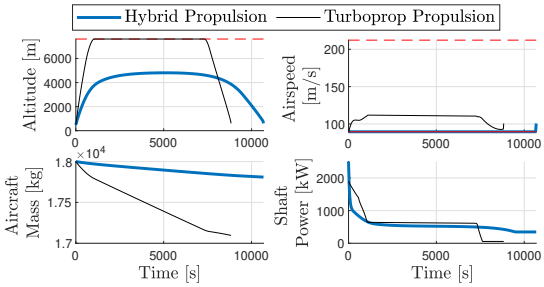


(a) Flight trajectories.

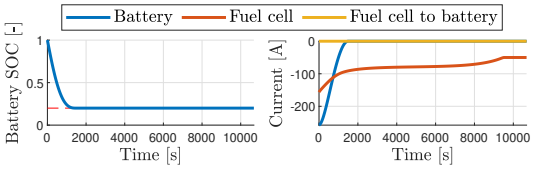


(b) Battery and fuel cell usage.

Fig. 3: Results for minimum propellant consumption problem.

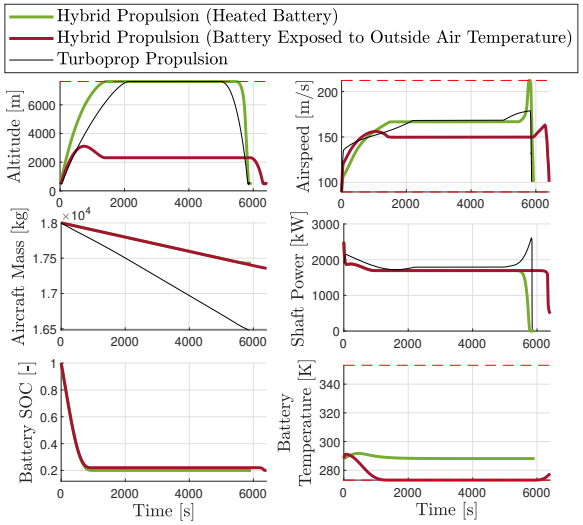


(a) Flight trajectories with and without battery heating.

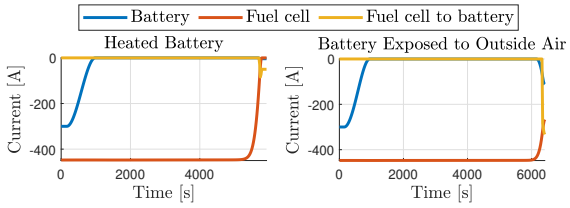


(b) Battery and fuel cell usage.

Fig. 4: Results for the minimum time problem, with and without heating of the battery.

### B. Results: Minimum Propellant Consumption Problem

The results for the minimum propellant problem are shown in Figure 3. As seen in Figure 3a, the optimal solution for the turboprop aircraft was to climb to the ceiling altitude to benefit from the decrease in air density and resistance for better efficiency. By contrast, the hybrid aircraft climbed to

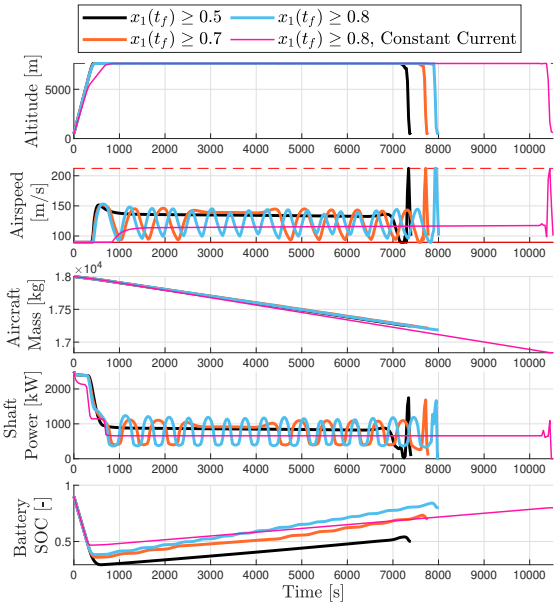


(a) Flight trajectories.

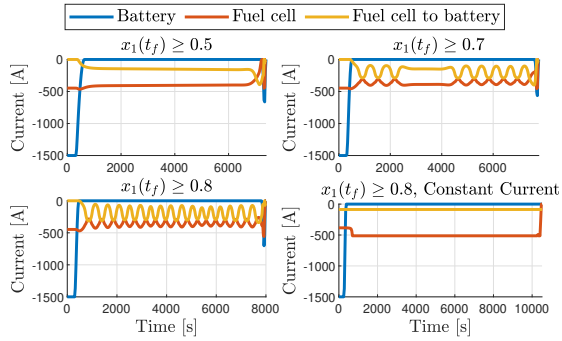


(b) Battery and fuel cell usage.

Fig. 5: Results for the fast climb and descend problem.

a lower altitude of approximately 5,000 m and travelled at a slower airspeed. Whilst the shaft power of both aircraft were similar, the mass of fuel burned by the turboprop was greater than that from the hybrid aircraft.

Figure 3b shows the distribution of the current across the hybrid power system during the flight. During the climb, most of the current is drawn from the battery to meet the power demands and to limit the burning of hydrogen fuel. Then, during the cruise stage when the battery has gradually reached its 20% state-of-charge limit, the hydrogen fuel cell dominates as the power source. Note that none of the current is used from the fuel cell to recharge the battery during the flight for this minimum consumption problem. This result agrees with [20] which, for a hybrid aircraft composed of a battery and a mechanical engine, found that only a minimal amount of fuel is saved by charging the battery during flight.

### C. Results: Minimum Time Problem

The results for the minimum time problem are shown in Figure 4. The comparison between the turboprop and the hybrid aircraft is shown in Figure 4a. Notice that the flight time is similar. The hybrid aircraft initially demanded more power and followed a fast climb, in contrast to the turboprop. The two aircraft then cruised at similar altitude and speed.

Figure 4b shows the response of the electric power system during this flight. The main difference compared to the minimum propellant problem of Figure 3b is that the current drawn from the fuel cell stack is significantly increased, and the battery drained faster. During descent, current from the fuel cell can be seen to be injected back into the battery.

As discussed in studies such as [11], the thermal response of the battery is an important for electric aircraft. Figure 4a compares the model predictions when the battery is insulated (as in when $T_{\text{amb}} = 293.15\,K$– this is referred to as the heated battery in Figure 4a) and when it is exposed to the outside air. The benefits of insulating the battery are clear from this figure. Without insulation, the heat generated by the battery is not enough to balance out the drop in ambient temperature as the aircraft climbs. As such, the insulated battery achieves a higher and faster cruise and reaches its destination sooner, highlighting the benefits of insulating the pack.

### D. Fast Climb and Descend Scenario

The solution to traditional trajectory optimisation problem formulations show that when full flexibility is given to adapt the flight trajectories, charging of the battery in flight is often unnecessary. However, there will also be scenarios where in-flight charging of the battery becomes an indispensable part of the real-world operations. Here, we consider a scenario where adverse weather is present at lower altitude of the flight path so that the aircraft should maintain at an the maximum altitude of 2,6000 ft as much as possible. For this problem, the objective becomes

$$\min_{x,u,t_f} \int_0^{t_f} s_h(t)^2 \, \mathrm{d}t + \lambda_t t_f + J_{\text{reg}} \tag{10}$$

with $s_h(t) \geq 0$ a slack variable for the path constraint $h(t) + s_h(t) \geq 7,620$ m. $\lambda_t = 0.01$ the trade-off parameter for the secondary objective to minimize the flight time. The scenario is further complicated by a short turn-around requirement (or lack of facilities) at the destination airport, requiring the SOC to be higher than a certain level at arrival. This scenario poses an interesting challenge for the operation of the hybrid electric aircraft:

- to reach a high altitude quickly, the energy stored in the battery must be consumed to allow a steep climb,
- the fuel cell must charge the battery in-flight to meet the arrival battery SOC requirement.

Figure 5 compares the results of solving this problem for different values of the final battery state-of-charge, with $x_1(t_f) \geq \{0.5, 0.7, 0.8\}$. When the required SOC of the battery can be reached through continuous charging using the excess energy from the fuel cell, e.g. in the case with $x_1(t_f) \geq 0.5$, a gradual increase in the battery SOC is observed after the initial climb and the aircraft maintains steady flight. As the final SOC requirement is increased, as in when $x_1(t_f) \geq 0.7$, 0.8, then oscillations emerge in the profiles of Figure 5 due to in-flight fast charging of the

battery. Here the trajectory of the aircraft oscillates between two operation points:

- One of the operation point corresponds to the optimal cruise condition of the aircraft. However, the excess power available from the fuel cell at this condition cannot continuously charge the battery to a level that is required at the end of the flight.
- The other operation point corresponds to the optimal charging condition of the battery by the fuel cell. However, under this condition, the available shaft power will not be enough for the aircraft to maintain its airspeed.

By switching between the two operation points, i.e. by switching between periods where the airspeed is allowed to drop for fast charging of battery, and periods where the charging current to battery is allowed to drop for the recovery of airspeed, the battery can achieve an overall faster charging rate in comparison to steady flight operations. This can be observed in Figure 5a with steeper SOC charging curves seen during the oscillations.

Figure 5 also presents the solution where $x_1(t_f) \geq 0.8$ is enforced together with $\mathrm{d}i_{fc2batt}(t)/\mathrm{d}t = 0$, i.e. requiring a constant current for the in-flight charge of the battery. This solution corresponds to the strategy that throughout the cruise, the split of the power remains relatively constant for the part that is used to power the flight and for the part that is used to charge the battery. In comparison to the solution with airspeed and current variations, this constant current solution is clearly sub-optimal: with longer flight time, higher propellant consumption, and a slower charging rate for the battery SOC.

In summary, imposing higher terminal SOC values causes a trade-off to be navigated between the power from the fuel cell that is siphoned off to charge the battery and that which is used to maintain the aircraft at its optimal flight trajectory. These results demonstrate that for flight scenarios with simultaneous requirements on the flight path and on the energy sub-system, the solution will be non-conventional and non-trivial. The need for in-flight charging also contrasts with the lack of in-flight charging identified in the earlier results for the minimum time and fuel consumption problems as well as that on [20], all based on having higher flexibility in the solution space for the flight trajectories.

## Conclusions

A method to optimise flight trajectories for electric aircraft powered by lithium-ion batteries and fuel cells was developed. Mathematical models for the aircraft, battery, fuel cell and motor were incorporated for the numerical solution of the resulting optimal control problems. Three problems were solved for a benchmark flight between London and Berlin involving an electrified Fokker 50 aircraft; a minimum propellant consumption problem, a minimum time problem, and one which prioritised the aircraft to remain at high altitude and the battery to be charged upon arrival. In all cases, the trajectories of the electric aircraft differed from that of a turboprop; for the minimum propellant problem, the electric aircraft flew with a faster but lower cruise whereas for the minimum time problem, the hybrid aircraft was faster but operated at higher shaft powers. Oscillations in the in-flight charging were observed for the high altitude flight problem with the battery charged upon arrival, with these oscillations caused by the balancing between the aircraft's propulsive needs and that required to charge the battery. The paper also explored the role of battery temperature on the response, providing a limit on aircraft performance. Future work will further enhance the realism of the modelling and problem formulation, and explore the benefits of electric aircraft co-design together with operation trajectories.

## References


[1] Aerospace Technology, "Fokker F-50 turboprop passenger airliner," *URL https://www.aerospace-technology.com/projects/fokker-f50/ (accessed Sep. 10, 2023)*, 2023.

[2] P. M. Attia, A. Grover, N. Jin, K. A. Severson, T. M. Markov, Y.-H. Liao, M. H. Chen, B. Cheong, N. Perkins, Z. Yang *et al.*, "Closed-loop optimization of fast-charging protocols for batteries with machine learning," *Nature*, vol. 578, no. 7795, pp. 397–402, 2020.

[3] J. T. Betts, "Survey of numerical methods for trajectory optimization," *Journal of guidance, control, and dynamics*, vol. 21, no. 2, pp. 193–207, 1998.

[4] A. Bills, S. Sripad, L. Fredericks, M. Guttenberg, D. Charles, E. Frank, and V. Viswanathan, "A battery dataset for electric vertical takeoff and landing aircraft," *Scientific Data*, vol. 10, no. 1, p. 344, 2023.

[5] A. Bills, S. Sripad, W. L. Fredericks, M. Singh, and V. Viswanathan, "Performance metrics required of next-generation batteries to electrify commercial aircraft," *ACS Energy Letters*, vol. 5, no. 2, pp. 663–668, 2020.

[6] M. Clarke and J. J. Alonso, "Lithium–ion battery modeling for aerospace applications," *Journal of Aircraft*, vol. 58, no. 6, pp. 1323–1335, 2021.

[7] Delft University of Technology, "Performance Model Fokker 50," Delft University of Technology, Tech. Rep., 2010.

[8] Department of Energy Security & Net Zero, "2022 UK greenhouse gas emissions, provisional figures," 30 March 2023.

[9] M. Doff-Sotta, M. Cannon, and M. Bacic, "Optimal energy management for hybrid electric aircraft," *IFAC-PapersOnLine*, vol. 53, no. 2, pp. 6043–6049, 2020.

[10] ——, "Predictive energy management for hybrid electric aircraft propulsion systems," *IEEE Transactions on Control Systems Technology*, vol. 31, no. 2, pp. 602–614, 2022.

[11] R. D. Falck, J. Chin, S. L. Schnulo, J. M. Burt, and J. S. Gray, "Trajectory optimization of electric aircraft subject to subsystem thermal constraints," in *Procs. of the Multidisciplinary Analysis and Optimization Conference*, 2017, p. 4002.

[12] M. Kaptsov and L. Rodrigues, "Flight management systems for all-electric aircraft," in *Conference on Control Technology and Applications (CCTA)*. IEEE, 2017, pp. 2126–2131.

[13] ——, "Flight management system for hydrogen-powered aircraft in cruise," *Aerospace Systems*, vol. 4, no. 3, pp. 201–208, 2021.

[14] J. Larminie, A. Dicks, and M. S. McDonald, *Fuel cell systems explained*. J. Wiley Chichester, UK, 2003, vol. 2.

[15] A. Misley, A. Sergent, M. D'Arpino, P. Ramesh, and M. Canova, "Design space exploration of lithium-ion battery packs for hybrid-electric regional aircraft applications," *Journal of Propulsion and Power*, vol. 39, no. 3, pp. 390–403, 2023.

[16] Y. Nie, O. Faqir, and E. C. Kerrigan, "ICLOCS2: Try this optimal control problem solver before you try the rest," in *Procs. of the United Kingdom Automatic Control Council (UKACC) International Conference on Control*. IEEE, 2018, pp. 336–336.

[17] Y. Nie and E. C. Kerrigan, "External constraint handling for solving optimal control problems with simultaneous approaches and interior point methods," *IEEE Control Systems Letters*, vol. 4, no. 1, pp. 7–12, 2020.

[18] G. Tucker, R. Drummond, and S. R. Duncan, "Optimal fast charging of lithium ion batteries: Between model-based and data-driven methods," *Journal of The Electrochemical Society*, vol. 170, no. 12, p. 120508, 2023.

[19] M. Wang, S. Kolluri, K. Shah, V. R. Subramanian, and M. Mesbahi, "Energy management for an all-electric aircraft via optimal control," *IEEE Transactions on Aerospace and Electronic Systems*, vol. 59, no. 2, pp. 1084–1095, 2022.

[20] M. Wang and M. Mesbahi, "To charge in-flight or not: A comparison of two parallel-hybrid electric aircraft configurations via optimal control," *IEEE Transactions on Transportation Electrification*, 2023.